# Emulsifiers of Pickering-like characteristics at fluid interfaces

Spyropoulos, Fotis; Clarke, Christopher; Kurukji, Daniel; Norton, Ian T.; Taylor, Phil

*DOI:*
10.1016/j.colsurfa.2020.125413

*License:*
Other (please provide link to licence statement

*Document Version*
Peer reviewed version

*Citation for published version (Harvard):*
Spyropoulos, F, Clarke, C, Kurukji, D, Norton, IT & Taylor, P 2020, 'Emulsifiers of Pickering-like characteristics at fluid interfaces: Impact on oil-in-water emulsion stability and interfacial transfer rate kinetics for the release of a hydrophobic model active', *Colloids and Surfaces A: Physicochemical and Engineering Aspects*, vol. 607, 125413. https://doi.org/10.1016/j.colsurfa.2020.125413

# Emulsifiers of Pickering-like characteristics at fluid interfaces: Impact on oil-in-water emulsion stability and interfacial transfer rate kinetics for the release of a hydrophobic model active

*Fotis Spyropoulos*[1*], *Christopher Clarke*[1], *Daniel Kurukji*[1], *Ian T. Norton*[1], *Phil Taylor*[2]

[1]School of Chemical Engineering, University of Birmingham, UK
[2]Formulation Technology Group, Syngenta Ltd, Jealott's Hill International Research Centre, UK

## Abstract

The influence of interfacial layer composition on the release kinetics of a model hydrophobic active (dimethyl phthalate, DMP) from oil-in-water (o/w) emulsions relevant to foods is reported. The present study considers various food-relevant emulsifiers known to form colloidal particles in aqueous solutions. These range from a low molecular weight surfactant and protein polyelectrolytes, to biopolymer complexes and solid particles: sodium stearoyl lactylate (SSL); bovine serum albumin (BSA); sodium caseinate (NaCAS), chitosan (Ch); BSA/Ch or NaCAS/Ch complexes; and silica (Pickering) nanoparticles (A200), were all investigated. In all cases, DMP release from the oil droplets of the o/w emulsions was controlled by the interfacial transport of the active rather than by its diffusion through the globules' interior. Release data followed first-order kinetics, where emulsions stabilised by soft (protein/polysaccharide complexes) colloidal structures were shown to provide similar (528 $nm^2\ s^{-1}$) or even lower interfacial rate constants (241 $nm^2\ s^{-1}$) to harder (silica) particulate entities (625 $nm^2\ s^{-1}$). SSL (a lamellar-phase forming surfactant that has been previously suggested to stabilise o/w emulsions via a mechanism closely resembling that of Pickering particles) exhibited the lowest interfacial release rate (17 $nm^2\ s^{-1}$). Overall, the present study contributes to current understanding on how emulsion interfacial architecture can be controlled to provide desirable molecular release performances.

## Keywords:

oil-in-water emulsions; Pickering stabilisation; interfacial transfer rate; sodium stearoyl lactylate; protein/polysaccharide complexes; silica nanoparticles.

[*] Corresponding Author: F.Spyropoulos@bham.ac.uk

# 1. Introduction

The encapsulation of functional ingredients is a key part of formulation science. Such functional species encompass flavour molecules; pharmaceuticals; nutraceuticals; coatings; agrochemicals; biologicals such as DNA, RNA, and peptides; and many more. Microstructure design for encapsulation invariably involves spatial and temporal control of the active ingredient(s) [1]. This may be employed to increase active stability, taste masking (e.g. peptide bitterness) [2], control delivery rates to biological targets, and/or to co-formulate otherwise physically disparate actives within the same liquid formulation [3],[4].

Emulsions offer a convenient template for encapsulation and controlled delivery of functional molecules due to their multi-phase components (oil, water, emulsifier). Emulsion composition/physical properties are defined by parameters including dispersed phase chemistry, emulsifier composition, and droplet size distribution. The material composition and processing route together determine the final microstructure, and this ultimately dictates the equilibrium and kinetic phenomena of dissolved functional material.

A typical interface occupies somewhere in the range 1-10 $m^2 g^{-1}$ depending on average droplet size and phase density. How emulsifiers impart stability has been (and still is) extensively studied across a wide range of interfacial species [5]-[7]; it is often a key performance indicator. However, to what extent emulsifier composition controls molecular release from the emulsion disperse phase is less understood. Of particular interest is the comparative difference between a typical polyelectrolyte (e.g. protein), a hard Pickering particle (e.g. silica) and softer particles such as those formed through biopolymer complexation. Often particulate interfaces are cited as providing a greater release barrier [5], however protein interfaces can often be preferable due to their diverse functionality, biodegradability and biocompatibility [7].

A major benefit of Pickering emulsions is their ability to offer a route to capsules with well-defined interfacial thickness and permeability. Disparate chemistries including fat crystals [8] and latex particles [9] have been utilised for this purpose. Simovic *et al.* [10] demonstrate sustained release of dibutyl phthalate from nanosilica stabilised emulsions at sodium chloride concentrations capable of causing partial interfacial flocculation. Frasch-Melnik *et al.* [11] reported controlled release of sodium chloride using tripalmitin-monoglyceride water-in-oil Pickering emulsions. Crystallisation at interfaces [10],[11] is an avenue for implementation to foods [12] and pharmaceuticals, since chemical functionalisation and/or use of hazardous reagents (e.g. glutaraldehyde, isocyanate, etc.) is not required [13],[14]. For products not designed for human consumption, interfacial cross-linking has found niche applications in agrochemical formulations (e.g. capsule suspensions) to impart specific functionality (UV protection or sustained release). Interfacial crosslinking of proteins and polysaccharides using chemical (e.g. glutaraldehyde and polyphosphate crosslinking of chitosan) [15] and enzymatic methods (e.g. laccase) [16] have been reported as applicable to foods and pharmaceuticals. Since their inception, emulsions stabilised via layer-by-layer (LbL) deposition or pre-formed complexes are cited to add value for controlled release [17]. Despite this, research exploring this area in an experimentally systematic manner is limited.

Based on the aforementioned gap in knowledge, this study aims to assess the capacity of a range of emulsifier species, that are relevant to food applications, to provide an interfacial barrier that regulates the release of an encapsulated model hydrophobic active (dimethyl phthalate; DMP) from oil-in-water (o/w) emulsions. Although the chosen emulsifier species differ substantially in their fundamental structures, they have also been shown, or are considered, to produce interfaces with properties akin to those stabilised by soft or hard particles. For example, while the low molecular weight surfactant sodium stearoyl lactylate has

been reported to possess a (liquid) crystalline structure in water [18], its action in emulsions (<42ºC) is claimed to provide a solid interfacial layer [19]. Other emulsifiers investigated include proteins (bovine serum albumin and sodium caseinate), and their biopolymer complexes formed with chitosan, which can produce soft colloidal particles that also possess the capacity to stabilise emulsions. These interfaces are compared to the hard particle interfaces created by hydrophilic silica (Aerosil® 200). Emulsions stabilised by all emulsifiers studied here were characterised in terms of their droplet sizes. DMP release from these systems (under sink conditions) was analysed using the model proposed by Washington and Evans [20] and it was shown to be limited by the transfer of the active across the droplet interface created, rather than by diffusion. DMP interfacial rate constants for all systems were calculated and it was demonstrates that interfaces stabilised by protein/polysaccharide complexes can provide an interfacial barrier of comparative or even enhanced functionality to one populated by typical Pickering particles.

# 2. Experimental

## 2.1. Materials

Sodium caseinate (NaCAS), bovine serum albumin (BSA), dimethyl phthalate (DMP), acetic acid, and low (50-190kDa) and medium (190-310kDa) molecular weight chitosan (LCh and MCh, respectively), both with de-acetylation degrees >75%, were obtained from Sigma Aldrich (UK). Hydrophilic nanosilica (Aerosil® 200; A200) was obtained from Evonik Industries (Germany). Sodium stearoyl lactylate (SSL) was kindly donated by Danisco (Denmark). Sunflower oil (SFO) was obtained from the local supermarket (Tesco, UK). Materials were used directly from the manufacturer without any further purification. Water was passed through a double-distillation column equipped with a de-ionisation unit. Concentrations (%) are reported as wt% (g/g) unless stated otherwise.

## 2.2. Methods

### *2.2.1. Preparation of emulsifier-containing aqueous phases*

The precise proportions and preparations of the emulsifier-containing aqueous phases are as follows:

i. *Sodium stearoyl lactylate* (SSL): A 1% SSL aqueous phase was prepared by dispersing bulk SSL powder into water at 50ºC under magnetic stirring; this resulted in an opaque solution/suspension containing lamellar SSL aggregates [21]. The suspension was left to stand at ambient temperature until it reached 20ºC.

ii. *Sodium Caseinate* (NaCAS): A 1% NaCAS aqueous phase was prepared in 30 mM sodium acetate buffer adjusted to pH 5 under magnetic stirring. At this pH, NaCAS has been found to exist as partly dewatered particles [22] which formed the desired insoluble complexes upon the addition of chitosan (see section *v*).

iii. *Bovine serum albumin* (BSA): A 1% aqueous solution of BSA was prepared by addition of BSA to a pH 5 sodium acetate buffer solution; the pH environment was selected to facilitate complexation with chitosan (see section *vi*). The solution was left to stir for approximately 2 hours prior to use.

iv. *Chitosan* (Ch): A stock solution of 1% chitosan (MCh or LCh) was prepared with water and acetic acid to pH 3, with required volumes taken and adjusted under vigorous stirring to pH 5 with 10% sodium hydroxide solution. This was to enable the formation of insoluble complexes when added to NaCAS or BSA aqueous phases at the same pH (see sections *v* and *vi*, respectively) [22].

v. *Sodium caseinate/chitosan complexes* (NaCAS/Ch): Equal quantities of aqueous phases of 1% NaCAS and 1% Ch (MCh or LCh) at pH 5 (see above preparations) were combined using magnetic stirring, spontaneously producing insoluble complexes. Suspensions were subjected to sonication (Viber Cell 750, Sonics, USA) using a 12 mm diameter probe for 2 minutes (20kHz, 95% amplitude). This method is described in detail elsewhere [22]. The Ch-to-protein fraction of the resulting NaCAS/Ch complexes was 1/1 and their (z-average) diameter was ~564 nm.

vi. *Bovine serum albumin/chitosan complexes* (BSA/Ch): BSA/Ch complexes were formed via two different processing methods, following the procedure reported elsewhere [22]. Regardless of the processing method employed, the Ch-to-protein fraction in the BSA/Ch complexes was 1/3. Briefly:

- METHOD 1 (M1). Under M1, 37.5 g of 1% Ch solution was added dropwise to 12.5 g of 1% BSA solution (both at pH 5) while stirring at 20ºC. Irrespective of Ch molecular weight (MCh or LCh), M1 yielded transparent dispersions/solutions with no discernible interface present between the biopolymer solutions, suggesting co-solubility. This is in agreement with [22] which concluded that BSA/Ch complexation following the M1 protocol yields soluble complexes.
- METHOD 2 (M2). For M2, Ch and BSA aqueous solutions (pH 5) of identical compositions as in M1 were combined as above, but the mixture was heated to 90ºC (above the denaturation temperature of BSA) [23] then cooled to ambient temperature (20ºC). The suspension was then sonicated using a 12 mm diameter probe for 2 min (20 kHz, 95% amplitude). Irrespective of Ch molecular weight (MCh or LCh), sonicating these aggregates yielded sub-micron sized complexes (~667 nm in diameter), as verified previously by dynamic light scattering [22]. This aligns with the findings of [22] which reported that BSA/Ch complexation following the M2 protocol yields insoluble BSA/Ch complexes.

vii. Aerosil® 200 *Silica* (A200): A200 was dispersed in 30 mM sodium acetate buffer at pH 2 (using 10% NaOH for the pH adjustment) to make a 1% suspension. 50 g of A200 (pH 2) dispersion were sonicated for 2 min at 95 % amplitude. This yielded a z-average particle diameter of ~150 nm, as measured by dynamic light scattering (DLS); this is in-line with previous work [24].

### *2.2.2. Preparation of o/w emulsions*

The emulsions comprised 20% oil phase and 80% aqueous phase. The oil phase was a solution of sunflower oil (SFO) and dimethyl phthalate (DMP) prepared in a weight ratio of 56:6 (SFO:DMP). The emulsifier composition was prepared in the emulsion aqueous (continuous) phase. All emulsions were produced by adding 40 g of the aqueous (emulsifier-containing) phase to 10 g of the oil phase and emulsifying using a Silverson rotor-stator mixer (Silverson Machines, UK) for 5 min at 6000 rpm and at room temperature.

### *2.2.3. Preparation of o/w LbL emulsion*

The layer-by-layer (LbL) approach involves the preparation of a primary protein-stabilised emulsion which is then diluted into an aqueous phase of an oppositely charged biopolymer; the pH of both is the same or is adjusted after mixing to promote electrostatic deposition at the interface. The LbL route was investigated only for the NaCAS/Ch system and compared against emulsions stabilised by preformed NaCAS/Ch complexes. To achieve this, a primary emulsion stabilised by 1% NaCAS was first prepared, before the addition of 1% Ch solution at pH 5, under either low shear (LS) magnetic stirring or high shear (HS) Silverson rotor-stator mixing (6000 rpm, 5 min).

### 2.2.4. Emulsion Characterisation

*Droplet size analysis.* Average droplet sizes were measured by laser diffraction using a Malvern Mastersizer 2000S (Malvern Instruments, UK) device equipped with a Hydro S dispersion cell. Because of the specific importance of emulsion droplet surface area to interfacial transport, average droplet diameters are reported as the volume-surface weighted mean diameters ($D_{3,2}$) rather than volume mean diameters ($D_{4,3}$).

*Interfacial tension (IFT).* Interfacial tension measurements were carried out following a slight variation to the protocol employed by Pichot *et al.* (2009) [25]. Briefly, IFTs were measured via the pendant drop method (Easydrop goniometer Krüss, Germany). Drops were aged to 3000 s, whereupon equilibrium IFT was reached; the only exception being A200. In this case, IFT continued to decrease (at a much significantly slower rate) after this time point, an effect that has been previously reported to be due to surface active impurities present in commercial sunflower oil [25]. As such, equilibrium IFT values for all systems reported here were obtained at a droplet age of 3000 s. The interfacial tension between distilled water and the used commercial sunflower oil was monitored throughout this work (at least on a weekly basis); the average equilibrium interfacial tension for this system was 24.61 ± 0.89 mN/m.

### 2.2.5. Release measurements

1 g of each DMP-containing o/w emulsion was transferred into cellulose dialysis tubing (10 mm × 150 mm, 14 kDa molecular cut-off), which was hydrated for 48 h prior to use. The emulsion-containing tubing was placed in 200 g of sodium acetate buffer (30 mM, pH 5) in a conical flask (the acceptor phase). Prior to the addition of the dialysis tubing, the acceptor phase was equilibrated to 20°C using a controlled water bath and was then on mildly mixed using a magnetic stirrer. The release was monitored by collecting 3 mL aliquots of the acceptor phase at regular time intervals over a total period of 6 h. The ultraviolet-visible (UV-VIS) absorbance (Libra S12, Biochrom, UK) of these samples was measured at a wavelength of 280 nm in a quartz cuvette. Using predetermined linear DMP calibration curves, the mass of active in the acceptor phase could then be determined. All release experiments were carried out within 48 h following emulsion preparation in order to ensure that destabilisation phenomena do not impact the measurements.

A schematic of the experimental dialysis membrane set-up is shown in Figure 1(I), where the transfer of active A from a single oil droplet, firstly to the continuous phase of the emulsion and then (after transferal across the dialysis membrane) to the acceptor phase, is depicted. The active is at a concentration of $[A]_o$ within the oil droplet (of volume $V_o$), $[A]_w$ in the continuous phase (of volume $V_w$) enclosed in the dialysis tube, and $[A]_{AP}$ in the acceptor phase (of volume $V_{AP}$); all quantities vary based on the rate of each transfer. As two interfaces are present (the droplet interface and the semi-permeable dialysis tubing) two rate constants must be considered. The rate constant $k_1$, describing release across the emulsion interface (the interfacial rate constant) into the continuous phase (with rate constant $k_{-1}$ being relevant to transferal in the opposite direction), and rate constant $k_2$, relating to molecular release from continuous phase of the emulsion to the acceptor phase (due to the imposed sink conditions, the reverse transfer rate constant $k_{-2}$ becomes practically zero). Preliminary testing demonstrated DMP adsorption onto the dialysis tubing to be insignificant, which contrasts previous work using dibutyl phthalate [10].

One potential issue with the release measurement set-up used here, as cited by Washington [26], is that the carrier phase (the emulsion droplet) does not experience a 'true' sink environment; i.e. the active does not experience its full driving force to release. This could lead to a situation where the molecular release kinetics are masked by partitioning phenomena;

i.e. measurement of an equilibrium feature, rather than a mass transfer coefficient [26]. Such a masking effect on release kinetics is in-line with a previous study which showed an inverse relationship between drug release rate and drug partition coefficient using the dialysis set-up [27]; in this study the release rate from the emulsion was governed by the amount of drug that was initially partitioned into the aqueous continuous phase, as dictated by the active's oil-water partition coefficient $K_p$ ($k_{-1}/k_1$). However, more recent work [27],[28] using model actives defined by reduced partition coefficients did not show an inverse relationship. This means that kinetic information can be obtained when using actives or model compounds of appreciable water solubility. In the present study different release rates were observed despite the use of the same active and oil phase, suggesting that the partition coefficient was not the only (or even a dominant) factor for delivery to the acceptor phase. What is more, DMP has an octanol-water partition coefficient ($K_{p,oct}$) of 33, which means that for o/w emulsions with a 20% oil phase, the percentage of total DMP partitioned into the continuous aqueous phase is predicted to be ~12%. This concentration may vary somewhat since the partition coefficient could have a slight interfacial area dependence [29], in addition to the difference in hydrophobicity between octanol and sunflower oil.

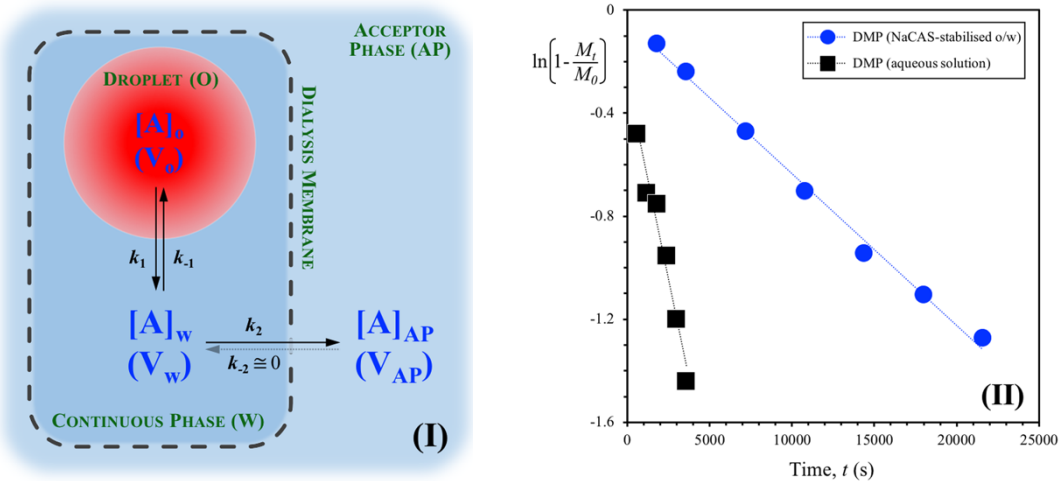


**Figure 1. (I)** Kinetic scheme for the dialysis membrane set-up used to measure the release rate of active A from o/w emulsions. $[A]_o$ and $V_o$, $[A]_w$ and $V_w$, and $[A]_{AP}$ and $V_{AP}$, are the concentration of the active in (and volume of) an oil droplet, the continuous phase of the emulsion, and the acceptor phase (sink). At equilibrium, the partitioning ($K_p$) of the active between the oil droplet ($[A]_o$) and the continuous phase ($[A]_w$) is governed by the ratio of the reverse and forward release rate constants ($k_{-1}/k_1$); $k_1$ is the interfacial rate constant. As the (emulsion-containing) dialysis membrane is placed within the acceptor phase, this equilibrium can be perturbed and the release of the active can also be affected by $k_2$. Concentration $[A]_{AP}$ is then assayed over time to generate the release profile. **(II)** First order fits to experimental data for DMP release from a NaCAS-stabilised o/w emulsion (blue circles) and an aqueous DMP solution (no emulsion; black squares). DMP concentration in the latter was half of the aqueous partitioning concentration; assumed to be that of octanol/water ($K_{p,oct} = 33$). For the emulsion, $M_t$ is equal to $[A]_{AP}$ at different times $t$, and $M_0$ is equal to $[A]_o$ at $t = 0$. For the DMP aqueous solution, $M_t$ is also equal to $[A]_{AP}$ at different times $t$, but in this case $M_0$ is equal to $[A]_w$ at $t = 0$.

In order to determine the extent to which the dialysis membrane influenced DMP release kinetics, the fastest DMP-releasing system in this study (a DMP-containing NaCAS-stabilised o/w emulsion) was compared against an aqueous solution of the active (no emulsion). In the latter case, DMP was dissolved in water at half its aqueous partitioning concentration (assumed against $K_{p,oct}$), and then placed in a dialysis bag and released into the acceptor phase under the exact same conditions used in the release experiments from emulsions. DMP release from these two systems is shown in Figure 1(II) as first order plots. The slope of the line in each case gives

a first order rate constant; for the no emulsion situation this would be the $k_2$ rate constant. The data presented in Figure 1(II) demonstrate that the slope for no emulsion is five-times greater than that for the release of DMP from the emulsion. This clearly suggests that the overall rate constant for DMP release from the emulsion droplets into the acceptor phase is primarily governed by the interfacial rate constant ($k_1$) and not by the rate of mass transfer across the dialysis membrane ($k_2$).

*2.2.6. Fractional Release profiles*

Cumulative fractional release (CFR) profiles for DMP are presented as a function of time *t*. CFR data are calculated as the fraction of the cumulative amount of DMP released at time *t* ($M_t$) over that released at infinite time ($M_0$):

$$\mathrm{CFR} = \frac{M_t}{M_0} \qquad \text{Eq. 1}$$

$M_t$ is essentially the total mass of active measured in the acceptor phase at time *t*, while $M_0$ is equal to the amount of active entrapped within the emulsion droplets at time $t = 0$.

*2.2.7. Release modelling*

Release of an active enclosed within emulsion droplets can be considered using two limiting models [20],[30]. The first relates to release phenomena that are predominantly driven by the diffusion of the active through the oil core of an emulsion droplet and towards the interface; active concentration along the droplet radius is in this case complex and time-dependent. It has been proposed [20] that when no interfacial hindrance is present, active release at long times is well approximated by:

$$\frac{M_t}{M_0} = 1 - \frac{6}{\pi^2}\exp\left(-\frac{\pi^2 D}{r^2}t\right) \qquad \text{Eq. 2}$$

or its linear form:

$$\ln\left(1-\frac{M_t}{M_0}\right) = \ln\left(\frac{6}{\pi^2}\right) - \frac{\pi^2 D}{r^2}t \qquad \text{Eq. 3}$$

where $M_t$ and $M_0$ retain their previous meanings as defined for Eq. 1, *D* is the diffusion coefficient of the active in the emulsion droplet, and *r* is the globule radius. Plotting the natural logarithm term on the left-hand side of Eq. 3 against time should give a straight line, the slope of which can be used to calculate the diffusion coefficient *D*. The second model however is relevant to release behaviour that is mainly dictated by the transfer of the active across the interfacial barrier around the emulsion droplet; under these circumstances the concentration of the active within the droplet is now independent of radial distance and uniform at any given time. A mathematical model describing the release of an active when transport across the droplet interface is the rate-limiting step has also been proposed [20] and its long-time approximation is given below:

$$\frac{M_t}{M_0} = 1 - \exp\left(\frac{-3k_1}{r^2}t\right) \qquad \text{Eq. 4}$$

where $k_1$ is the interfacial rate constant; all other symbols retain their previous meanings. Eq. 4 can be rearranged to give:

$$\frac{r^2}{3}\ln\left(1-\frac{M_t}{M_0}\right) = -k_1 t \qquad \text{Eq. 5}$$

and plotting the term on the left-hand side against time *t* should yield a straight line, the slope of which can be used to directly calculate $k_1$.

DMP release from the emulsions studied in this work was expected to be dominated by transferal of the active across the emulsion interface and as such it should fall under the considerations within the second of these two models. Fitting the DMP data from the slowest and fastest active-releasing emulsion systems (SSL- and NaCAS-stabilised o/w emulsions, respectively) resulted in diffusion coefficients of $5.14 \times 10^{-18}$ and $5.64 \times 10^{-16}$ $m^2$ $s^{-1}$, respectively. However, at least in theory, these values should be equivalent as they both describe the same phenomenon, i.e. the diffusion of DMP within the same material (sunflower oil), and are normalised to exclude effects arising from differences in the size of the domains (droplets) within which diffusion takes place. Moreover, both these values are significantly lower to the diffusion coefficient for DMP within sunflower oil (a relatively small molecule diffusing through a liquid phase of moderate viscosity) as calculated using the Stoke-Einstein equation ($8.5 \times 10^{-12}$ $m^2$ $s^{-1}$). As such, the diffusion-limited model is not applicable to describe the release behaviour observed in this study and instead DMP data (at longer times; $t \geq 2$ h) were fitted to the model assuming that overall transport of the active is controlled by the nature of the interfacial layer (Eq. 5); best-fit parameters were used to calculate the interfacial rate constants $k_1$ for the discharge of DMP from all o/w emulsion studied in the present work.

#### *2.2.8. Statistical analysis*

All data are presented as mean values ± one standard deviation (SD). Statistical significance was determined by performing Student's t-test. Results were considered statistically significant at $p$-values $\leq 0.05$.

## 3. Results and Discussion

### 3.1. Emulsion interface, droplet size and stability

The first part of this work considers the effects of emulsifier adsorption on the interface, droplet size and stability of a range of formed o/w emulsions. A range of emulsifiers were studied here; although these differ in terms of their fundamental structures, they have also been shown to form (under the conditions used in this work) colloidal species that are expected to produce emulsion interfaces with properties akin to those stabilised by hard/solid particles. For all these systems, the relationship between interfacial tension and droplet size as well as two-month stability against droplet-droplet coalescence are presented. The emulsions were also observed for flocculation and creaming, phenomena that are both discussed where relevant; no specific attempts were made to control either of these.

#### *3.1.1. The effect on interfacial tension and emulsion droplet size*

Figure 2 presents the $D_{3,2}$ and equilibrium IFT data for each emulsifier composition. SSL facilitated the smallest average droplet size despite having a comparatively high IFT (~14 mN $m^{-1}$) relative to the other emulsifiers. This was likely due to the higher adsorption rate of SSL at the droplet interface, which during the high shear rate process of emulsification could be expected to provide a faster rate of IFT reduction and thus smaller droplets. Low molecular weight surfactants like SSL are well known to exhibit fast adsorption relative to larger polymers, biopolymer complexes and other colloidal species [31]. SSL has also been postulated to be present in the form of bi- or multilayer aggregates such as lamellas, where the comparatively high equilibrium interfacial tension has been previously explained with reference to this self-assembly [21]. The high IFT is likely to be due to a reduction in cohesive packing energy relative to other anionic and non-ionic surfactants. Sodium dodecylsulfate or Tween 20, for instance, lower the oil-water IFT to 1-5 mN $m^{-1}$ [32],[33].

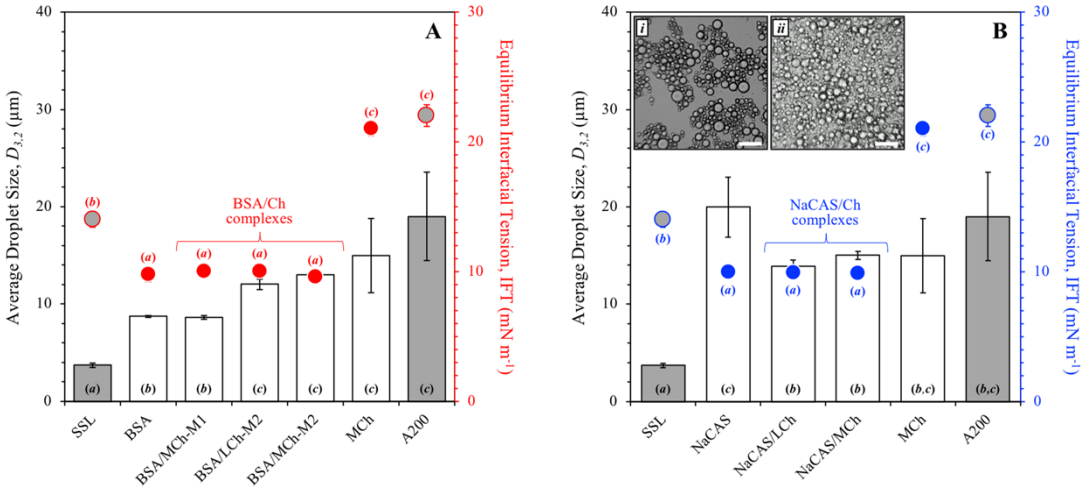


**Figure 2.** Average droplet sizes ($D_{3,2}$) of o/w emulsions (bars) stabilised by different emulsifiers and corresponding equilibrium interfacial tension (IFT) data (circles). **A.** o/w emulsions stabilised by BSA, MCh and BSA/Ch complexes. **B.** o/w emulsions stabilised by NaCAS, MCh and NaCAS/Ch complexes. SSL- and A200-stabilised o/w emulsions are also presented for comparison. Differences between data marked with the same letter are not statistically significant ($p > 0.05$). Inset micrographs showing o/w emulsions stabilised by NaCAS (*i*) and NaCAS/MCh complexes (*ii*) immediately after formation; scale bar is 60 µm.

Emulsifier compositions containing BSA or NaCAS give ~4 mN m$^{-1}$ lower IFT than SSL with both reaching similar values (~10 mN m$^{-1}$). BSA is a globular protein with an isoelectric point at ~pH 4.9 [34]. BSA self-association taking place near its isoelectric point (pH 5) has been shown to yield colloidal protein aggregates with dimensions of ~650 nm in diameter [34]. However the impact of the protein on the oil/water interfacial tension as a function of pH is minor. Ghosh and Bull [35] reported that a 0.06% BSA concentration at the water/*n*-octadecane give interfacial tensions of 19.4 and 18.2 mN m$^{-1}$ at pH 6.3 and pH 4.95, respectively. Although at higher protein concentrations (such as those studied here) BSA interfacial tension is further reduced, the low pH sensitivity remains. NaCAS, possesses a disordered structure and although typically associates into spherical micelles of 20–40 nm in diameter under neutral and weakly basic conditions, it can form colloidal particles of dimensions in the order of 200–300 nm at more acidic conditions (pH 5.1) [36] closer to its isoelectric point (~pH 4.2) [37]. Sodium caseinate partial aggregation could explain the higher equilibrium IFT values measured here (at pH 5) compared to those reported for the protein (~3 mN m$^{-1}$) at its native pH (pH ≈ 6.8) [38]. BSA/Ch and NaCAS/Ch complexes appear to closely follow the IFT reduction caused by their protein components [22]; statistical analysis confirmed that no significant difference ($p > 0.05$) in terms of equilibrium IFT exists between proteins and their equivalent complexes with Ch (Figure 2). Nonetheless, the droplet sizes for emulsions stabilised by proteins or their complexes with Ch do exhibit some variation. BSA- and BSA/MCh-M1-stabilised emulsions possessed practically indistinguishable droplet sizes, while systems formed in the presence of the BSA/LCh-M2 or BSA/MCh-M2 complexes had larger dimensions. It is suggested that the change in droplet sizes primarily relates to the soluble nature of BSA/Ch complexes produced via the M1 processing protocol, as oppose to the insoluble characteristics of those delivered in M2 [22]. On the other hand, droplet sizes stabilised by either of the two NaCAS/Ch complexes were not statistically different. Similarly to the BSA/LCh-M2- and BSA/MCh-M2- stabilised systems, Ch molecular weight in the NaCAS/Ch complexes does not appear to affect emulsion droplet size, providing complexation has been carried out according to the same procedure. NaCAS/Ch-stabilised emulsions though are smaller in comparison to systems formed in the presence of NaCAS alone. The latter systems however did exhibit evidence of flocculation soon after formation; see inset micrograph (*i*) in Figure 2B. Flocculation in o/w emulsions

stabilised by NaCAS/Ch complexes has also been reported to take place, but such events are significantly reduced for biopolymer assemblies with Ch-to-protein fractions equal or greater to 1/1 [22]. This was confirmed for the emulsions stabilised by NaCAS/Ch complexes in the present study (Ch-to-protein fraction of 1/1); see inset micrograph (*ii*) in Figure 2B.

In agreement to the data presented here, both MCh (pH 5) [39] and A200 (pH 2) [25] have been shown previously to give relatively high IFT values at the oil/water interface. As a result, both MCh- and A200-stabilised emulsions exhibited the largest final droplet sizes. Despite their deficiency to lower IFT, both species were able to produce o/w emulsions with no free oil phase observed (at 20% oil incorporation). In most cases polysaccharides are not efficient emulsifiers, with notable exceptions including gum-arabic (beverages) and sugar-beet pectin [40]. Chitosan is largely hydrophilic and has been shown to form a network of polyelectrolytic brushes on the water (continuous phase) side of o/w emulsions, thus providing significant steric stabilisation [39]. The emulsifying ability of chitosan depends on pH, where emulsification is facilitated at a pH closer to the amine pKa of chitosan (~6.5-7.0) but low or high enough such that phase separation does not ensue [41]. This was also confirmed in the present study, where the emulsifying capacity of chitosan at pH 5 was all but absent at pH 3.

### *3.1.2. The effect on emulsion stability*

Stability is a key performance attribute of any emulsion-based product. All o/w emulsions produced in this study were stored at 20ºC and 40ºC. Changes to droplet size distribution data were monitored over a month in order to determine variances in coalescence rates between systems stabilised by different emulsifier species.

The evolution of the average volume-surface weighted droplet size data ($D_{3,2}$) of o/w emulsions stored over a one month period at 20ºC is presented in Figure 3. With the exception of MCh, emulsions stabilised with single emulsifiers (*i.e.* SSL, BSA, NaCAS, or silica) exhibited minimal changes to their original droplet sizes. This shows that these emulsifiers confer stability to coalescence, with little anticipated change in the structure of droplet interfaces over time. Even the NaCAS-stabilised emulsions, which as discussed earlier did initially displayed some level of flocculation, where able to maintain a constant droplet diameter; although it has been reported that the emulsion structure of these systems collapses at ~ pH 4.5 [37]. Ch-stabilised emulsions were the only structures that fully collapsed after one month of storage and were thus unmeasurable. It should be noted that all emulsions prepared in this work exhibited creaming, albeit at different rates. All had appeared to have fully creamed after the one-month storage time; with the exception of SSL, which displayed turbidity in its lower phase suggesting the presence of droplets and/or non-adsorbed emulsifier.

Aside from systems formed only in the presence of MCh, emulsions stabilised by protein/chitosan biopolymer complexes exhibited the highest degree of droplet size changes over the quiescent storage period at 20ºC (Figure 3). During laser diffraction measurements, the recorded size data could potentially arise from droplet flocs. If the interaction forces stabilising the flocs can withstand the shear forces exerted within the dispersion unit of the measurement device, then the resulting droplet size measurement will be indicative of flocs. This behaviour has been described in previous studies with emulsions, ultimately reporting that measurement errors as a result of the phenomenon are significantly higher than for non-flocculated systems [42]. It has been observed that emulsions stabilised with mixed biopolymer films are prone to flocculation resulting from bridging of the biopolymers across the droplets [6],[42]. Visualisation (using light microscopy) of the emulsions stabilised by protein/Ch complexes in this work after only a few days of storage also revealed floc formation. However, examination of these systems (protein/Ch-stabilised emulsions) directly after emulsification using microscopy and droplet size measurements, did not show signs of flocculation, thus

suggesting that the phenomenon is exacerbated by creaming (and the close contact of droplets present within the formed cream layer) and the use of an anti-settling agent could potentially ameliorate this issue. In order to test this hypothesis, o/w emulsions stabilized by BSA/LCh-M2 or NaCAS/LCh complexes were stored (immediately after production) under gentle mixing (inhibiting creaming) at 20ºC and their droplet sizes were monitored over a period of nine days; Figure 4 presents the average droplet sizes measured throughout this time. The data clearly demonstrates that, in contrast to their quiescently stored counterparts, both these systems maintain their initial average droplet sizes, thus confirming that restricting droplet-to-droplet contacts (which are otherwise maximized when the globules are present at a cream layer) by gentle agitation essentially eliminates flocculation.

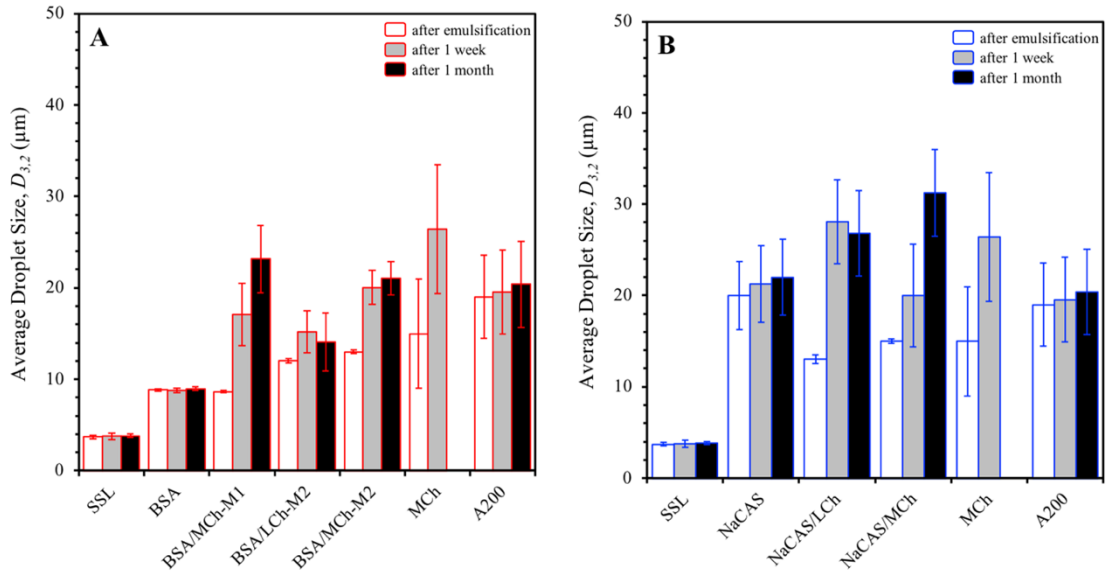


**Figure 3.** Evolution of the average droplet sizes ($D_{3,2}$) of o/w emulsions stabilised by different emulsifiers over a one month storage period at 20ºC. **A.** o/w emulsions stabilised by BSA, MCh and BSA/Ch complexes. **B.** o/w emulsions stabilised by NaCAS, MCh and NaCAS/Ch complexes. SSL- and A200-stabilised o/w emulsions are also presented for comparison.

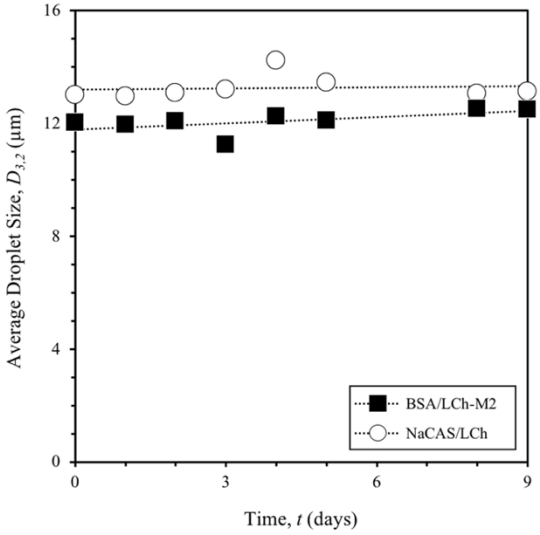


**Figure 4.** Evolution of the average droplet sizes (D3,2) of o/w emulsions stabilised by either BSA/LCh-M2 or NaCAS/LCh protein/chitosan complexes and stored under gentle mixing for 9 days. Best-fit lines to the data for each system are only shown to guide the reader's eye.

The o/w emulsions shown in Figure 3 were also stored for one month at 40ºC in the presence of 0.03% sodium azide ($NaN_3$) to limit microbial activity. The trends in terms of emulsion stability at 40ºC were comparable to those for systems stored at 20ºC with one important difference; the microstructure of the SSL-stabilised o/w emulsion fully collapsed (complete phase-separation) after one week of storage. It has been previously shown [21] that sunflower oil-in-water emulsions stabilised by SSL exhibit a melting transition at ~42ºC (equivalent to that of bulk SSL; 44.2ºC) but recrystallise at a much lower temperature of ~25ºC (significantly below that of bulk SSL; 43.2ºC). As such, it is clear that the crystalline structure of SSL confers its emulsions a great level of stability which practically disappears at temperatures that promote the transition of these structures into a liquid-like state.

### *3.1.3. Layer by Layer (LbL) Emulsions*

In the biopolymer-stabilised emulsions discussed so far in this study, protein/polysaccharide complexation was performed prior to emulsification; i.e. pre-fabricated complexes were used to stabilise the emulsions. However, another approach often described in literature [17],[43] involves adding the biopolymers to a pre-formed emulsion in a sequential manner; this is collectively known as layer-by-layer (LbL) deposition. This methodology has been previously demonstrated to generate emulsions with modified physicochemical properties, such as improved stability to heat [17] and freeze-thaw cycles [43]. However, the final volume fraction of the dispersed phase in LbL emulsions produced in this way is typically low (0.1-1%), as otherwise widespread flocculation (most commonly bridging flocculation) phenomena can take place upon addition of the secondary biopolymer to the primary emulsion [17].

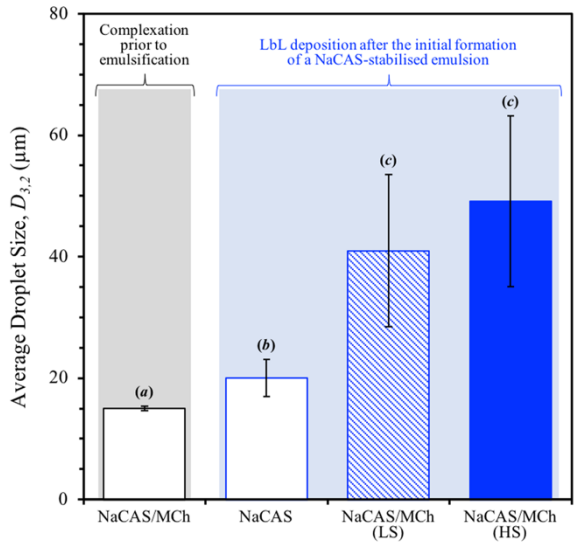


**Figure 5.** Average droplet sizes ($D_{3,2}$) of o/w emulsions stabilised by NaCAS/MCh complexes (formed prior to emulsification) and those stabilised by layer-by-layer (LbL) deposition of MCh at low shear (LS) and high shear (HS) following the initial formation of a NaCAS-stabilised o/w emulsion. Differences between data marked with the same letter are not statistically significant ($p > 0.05$).

Here, the LbL method was only tested for the NaCAS-MCh system and the resulting emulsions were compared against those stabilised by (preformed) NaCAS/Ch complexes. Investigation of NaCAS-Chitosan stabilised LbL emulsions indicated a large and statistically significant ($p > 0.05$) increase in measured droplet sizes (upon formation) as compared to the dimensions of either their protein-stabilised precursors or those of equivalent systems formed in the presence of NaCAS/Ch complexes (see Figure 4). As determined by light microscopy, this large increase in apparent droplet size was indicative of flocculation rather than

coalescence events, specifically occurring following the MCh deposition step. What is more, the data suggests that there is no statistical difference ($p > 0.05$) in the 'perceived' (due to flocculation) droplet (or floc) dimensions produced by carrying out the deposition of MCh within a low or high shear environment (Figure 5). This demonstrates that whilst the overall concentration of each of the biopolymers added to the emulsions can be equivalent for each processing method, the result in terms of microstructure formation is very different. Preformed complexes appear to possess the advantage of limiting flocculation phenomena during high shear mixing (emulsification); an important consideration that is all the more relevant for the large-scale manufacture of such emulsions.

### 3.2. The role of emulsifier on DMP release kinetics

The data for the cumulative fractional DMP release from o/w emulsions stabilised by either BSA, NaCAS, MCh, or selected BSA/Ch and NaCAS/Ch complexes are shown in Figure 6; DMP release from SSL- or A200-stabilised emulsions are also shown for comparison. Overall, the release profiles for all systems varied between those for the SSL-stabilised emulsion, which demonstrates the most sustained DMP release (35% released in 6 hours), and NaCAS, which released 70% of its payload within 6 hours. DMP cumulative fractional release data (at longer times; $t \geq 2$ h) for all studied emulsions were fitted to Eq. 5 (Figure 7); droplet radii were taken as half of the (previously obtained) corresponding $D_{3,2}$ values. The gradient of the produced linear fits (in all cases with $R^2 \geq 0.97$) is equal to $-k_1$; which allowed the calculation of rate constants for the transferal of DMP across o/w emulsion interfaces stabilised by a range of emulsifier species (Table 1).

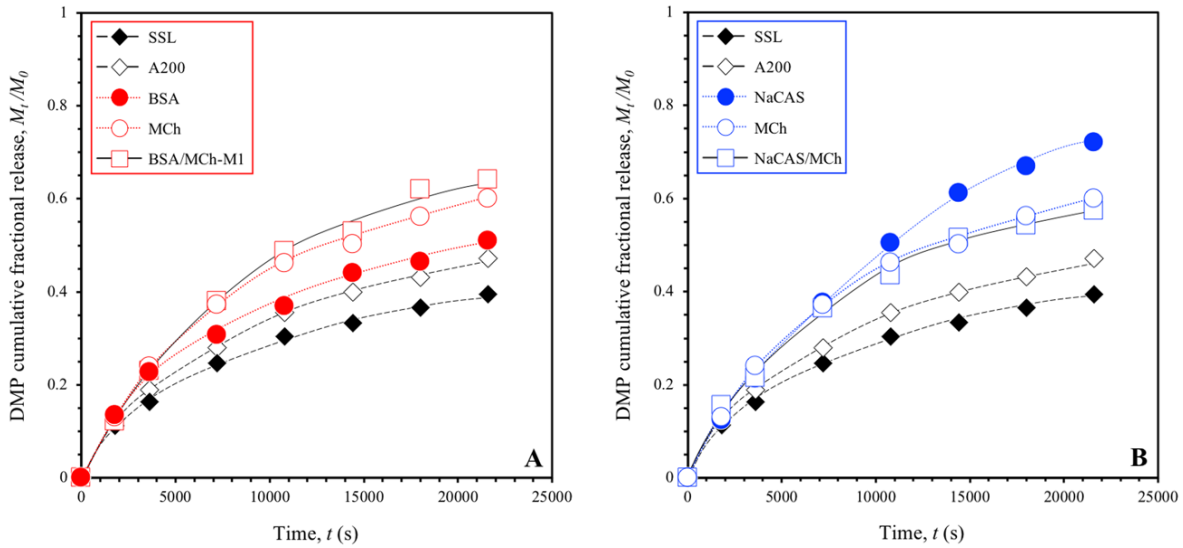


**Figure 6.** Dimethyl phthalate (DMP) cumulative fractional release profiles from o/w emulsions stabilised by: **A.** BSA, MCh, or their BSA/MCh-M1 complexes, and **B.** NaCAS, MCh, or their NaCAS/LCh complexes. In both cases, DMP cumulative fractional release profiles from o/w emulsions stabilised by SSL or A200 are also shown for comparison. Curves shown to guide the reader's eye.

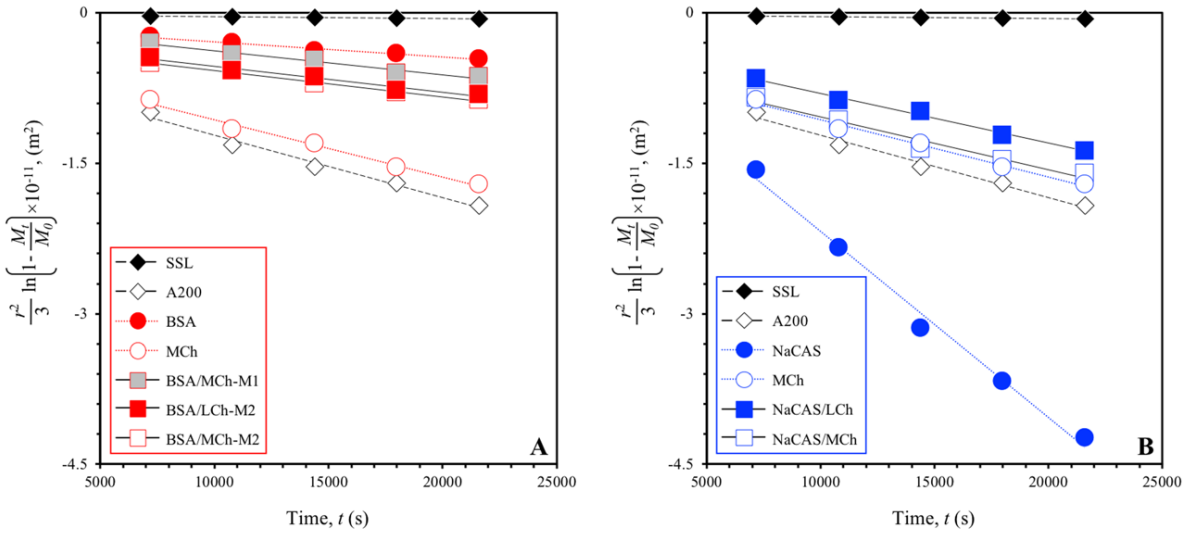


**Figure 7.** First order fits to data (for times $t \geq 2$ h or 7200 s) for the dimethyl phthalate (DMP) cumulative fractional release from o/w emulsions stabilised by: **A.** BSA, MCh, or their complexes, and **B.** NaCAS, MCh, or their complexes. In both cases, first order fits to data for DMP cumulative fractional release from o/w emulsions stabilised by SSL or A200 are also shown for comparison. Lines shown are best fits to Eq. 5.

| | $k_1 \pm$ SD (nm$^2$ s$^{-1}$) | $R^2$ |
|---|---|---|
| **SSL** | 17 ± 2 $^a$ | 0.986 |
| **BSA** | 153 ± 19 $^b$ | 0.982 |
| **NaCAS** | 1855 ± 161 $^f$ | 0.991 |
| **MCh** | 575 ± 53 $^e$ | 0.990 |
| **BSA/MCh-M1** | 241 ± 37 $^c$ | 0.974 |
| **BSA/LCh-M2** | 262 ± 21 $^c$ | 0.992 |
| **BSA/MCh-M2** | 260 ± 37 $^c$ | 0.977 |
| **NaCAS/LCh** | 497 ± 45 $^d$ | 0.991 |
| **NaCAS/MCh** | 528 ± 89 $^{d,e}$ | 0.967 |
| **A200** | 625 ± 72 $^e$ | 0.985 |

**Table 1.** Interfacial rate constants ($k_1$) calculated by fitting experimental data for the release of dimethyl phthalate (DMP) from o/w emulsions stabilised by different species, to Eq. 5; differences between $k_1$ values marked with the same superscripted letter are not statistically significant ($p > 0.05$). SD: Standard Deviation.

### *3.2.1. Interfaces stabilised by SSL or proteins*

Rate constants $k_1$ for all systems varied by almost two orders of magnitude from 17 nm$^2$ s$^{-1}$ for the o/w emulsion exhibiting the slowest DMP release (SSL-stabilised emulsion) to 1857 nm$^2$ s$^{-1}$ for the system with the fastest release (NaCAS-stabilised emulsion). There was a 10-fold difference in the $k_1$ values between the slowest two systems (SSL and BSA) and then an equally large variance in the emulsions exhibiting the second slowest (BSA) and highest overall (NaCAS) interfacial rate constants. This suggests that there is an interfacially-relevant structural feature in the SSL-stabilised o/w emulsions that gives rise to a significant retardation of DMP molecular release, relative to all other systems. In previous work [21], SSL was shown to produce a highly structured emulsion interface containing bilayer aggregates at room temperatures (20ºC), which are hypothesised control the slow DMP release rates measured here.

In terms of the protein-stabilised emulsions, BSA-only systems exhibited slower DMP release kinetics to those formed in the presence of NaCAS. Barbosa *et al*. [44] have shown that BSA retains its globular structure unaltered at pH 4.0 up to 9.0 (and at concentrations relevant to those used here) without any significant conformational change. It has been also previously demonstrated by interfacial rheology experiments that BSA forms more compact elastic surface films originating from its globular structure [45]. This would indicate that the globular structure of BSA, although potentially losing at least part of this higher order structure upon adsorption, creates a denser and higher (DMP) release energy barrier than NaCAS. What is more, if the aggregates that both proteins are expected to form at pH 5 persist during emulsification and take part in the interfaces created, then their dissimilar dimensions could potentially give rise to barriers of different thicknesses, with the BSA larger colloidal structures thus expected to more efficiently retard active migration [34],[36].

The values of interfacial rate constants determined here are largely within the same range of values reported in other (albeit limited) literature. Washington and Evans [20] obtained release rates of model acidic solutes (cupric, caprylic, and arachidic acid) from submicron triglyceride emulsions (d < 200nm) using a range of poloxamer and poloxamine block copolymer emulsifiers and lecithin. Interfacial rate constants determined in this study were within the range of 0.29 - 610 $nm^2\ s^{-1}$, with the release of arachidic acid from Pluronic F68-stabilised emulsions and that of chlorpromazine from lecithin-stabilised systems, giving the lowest and highest $k_1$ values, respectively [20].

In an attempt to further explore the large difference in the transport rates of surfactant- and protein-stabilised interfaces, the activation energy ($E_A$) for DMP release from an SSL emulsion droplet layer was determined following an Arrhenius approach and compared to the equivalent $E_A$ value for systems stabilised by BSA; this approach has been previously used to study the mechanism of molecular release from emulsions [10],[20]. DMP release measurements from emulsions stabilise by either of the two emulsifiers were carried out at different temperatures (20, 30, 40, 50, and 60ºC) and in each case the resulting interfacial constants $k_1$ were calculated. If an Arrhenius relationship exists, plotting the natural logarithm of these $k_1$ values (at each temperature $T$) as a function of $1/T$ should produce a straight line of slope equal to $-E_A/R$; where $E_A$ has units of J $mol^{-1}$ and $R$ (J $mol^{-1}\ K^{-1}$) is the gas constant. Deviation from linearity gives information about the mechanism of release; for example, a change in interfacial composition or structure (*e.g.* hydration or desorption of particles) as a function of temperature [10].

The Arrhenius plots for the release of DMP from SSL- and BSA-stabilised o/w emulsions are presented in Figure 8. In the case of BSA, the relationship between $\ln k_1$ and $1/T$ exhibits good linearity with a calculated $E_A$ value of 37 kJ $mol^{-1}$. Following the same process, the activation energy for DMP transport across the SSL-stabilised interface was calculated at 85 kJ $mol^{-1}$; clearly suggesting that SSL provides a greater barrier to DMP release than BSA. What is apparent in this case however is that the linear correlation applied across the full temperature range (20-60ºC) is somewhat disturbed above 40ºC. Moreover, SSL and BSA data >40ºC appear to more or less overlap. If these two linear portions are considered separately then $E_A$ values of 68.8 and 45 kJ $mol^{-1}$ can be determined for the 20-40ºC and 50-60ºC temperature regions, respectively. This temperature-induced deviation from the initial Arrhenius behaviour and the close alignment of this shift to the melting temperature for SSL (42ºC), further reinforce the hypothesis that the unique interfacial structure of this emulsifier controls release.

Interfacial activation energies determined here align well with those reported in literature for the release of small hydrophobic actives from emulsions or other relevant colloidal

structures. A study of guanosine release from polyethylene glycol-modified liposomes reported an increase in the activation energy required for the transport of the active across the lipid bilayer from 14 to 22 kJ mol$^{-1}$ [46]. In emulsions stabilised by Pluronic F-68, capric acid release was associated with an $E_A$ value of 52.8 kJ mol$^{-1}$ [20]. In another study, dexamethasone release from composites consisting of polylactic-co-glycolic acid microspheres coated with poly(vinyl alcohol) gave an activation energy of 116 kJ mol$^{-1}$ [47]. Finally, work [10] investigating the release of dibutyl-phthalate from polydimethylsiloxane-in-water emulsions stabilised by hydrophobic nanosilica particles, reported much higher $E_A$ values of 580 and 630 kJ mol$^{-1}$; at NaCl concentrations of $10^{-3}$ and $10^{-1}$ M, respectively. The authors propose that under these salt concentrations, a thick multilayer coating of fully aggregated hydrophobic silica nanoparticles (at $10^{-3}$ M NaCl) or a thick interfacial wall of hydrophobic nanoparticles (at $10^{-1}$ M NaCl) is expected to be formed, and conclude that such nanoparticle coatings offer a more significant barrier for molecular transport from emulsion droplets than adsorbed polymer layers [10].

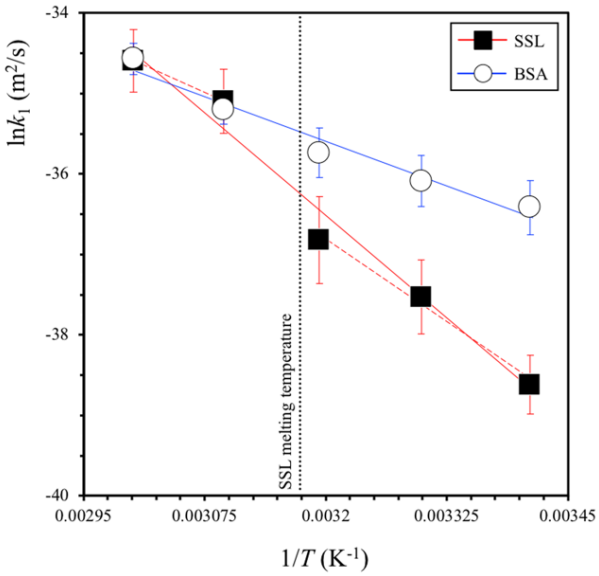


**Figure 8.** Arrhenius plots for the release of DMP from SSL- and BSA-stabilised o/w emulsions; solid lines represent best-fits to experimental data. In the case of SSL-stabilised o/w emulsions, separate linear fits to data above and below the melting temperature of the emulsifier (~42ºC; dotted line) are also presented as dashed lines (red).

### *3.2.2. Interfaces stabilised by protein/chitosan complexes or hydrophilic silica particles*

Overall, the interfacial rate constants for DMP release from emulsions stabilised by BSA/Ch complexes were found not to be statistically dissimilar ($p \leq 0.05$) from one another, with $k_1$ values in between those determined for either of the corresponding BSA- and Ch-only stabilised systems (Table 1). As such, no significant effects arisen from changes in the complexation method (M1 or M2) and/or the molecular weight of the Ch utilised. Despite the larger proportion of Ch-to-protein (3/1) in the formed complexes, interfacial transport of DMP appears to be principally controlled by BSA. On the contrary, although the $k_1$ values for the release of DMP from emulsions stabilised by NaCAS/Ch complexes were also found to be very comparable and similarly not sensitive to Ch molecular weight ($p \leq 0.05$), interfacial transport was shown to be more akin to that of Ch alone rather than the protein-only systems (Table 1). It might be that the higher fraction of Ch-to-protein in these systems (1/1) amplifies the polysaccharide contribution much more so than in the case of BSA/Ch complexes (Ch-to-protein fraction of 3/1). However, a different hypothesis could be put forward suggesting that

interfacial rate constants of such complexes are more extensively influenced by their constituent that possess the highest capacity to lower $k_1$ when used by itself; which is the BSA component for the BSA/Ch complexes and the Ch constituent for the NaCAS/Ch structures.

A study [10] on the release of dibutyl-phthalate (DBP) from o/w emulsions stabilised by either hydrophilic or hydrophobic silica nanoparticles reported (only for systems stabilised by hydrophobic silica; Aerosil® R974) very low $k_1$ values; 0.3 $nm^2\ s^{-1}$ and 0.05 $nm^2\ s^{-1}$, at NaCl concentrations of $10^{-3}$ and $10^{-1}$ M, respectively. These values are significantly lower than the rate constants determined in the current study for hydrophilic silica (Aerosil® 200) stabilised interfaces. However, analysis by the present authors of the data presented for emulsions stabilised by hydrophilic particles (Aerosil® 380) in the same study [10], reveals an interfacial rate constant of 15.3 $nm^2\ s^{-1}$; although still lower, it is much more in line with the findings reported here. The main reasons hypothesised to account for this difference are the smaller emulsion droplet sizes studied in [10] and the higher hydrophobicity of DBP; DBP has an octanol/water partition coefficient of 4.68 and an aqueous solubility of 1.0 mg/100 mL [10], while for DMP these are 33 and 0.43 g/100 mL, respectively.

It is worth noting that the $k_1$ values for all BSA/Ch and only the NaCAS/LCh complexes were lower than the interfacial rate constants determined for the silica-stabilised systems; no statistical difference was found in the case of the NaCAS/MCh complexes ($p \cong 0.066$). Besides the obvious differences in the dimensions of the two classes of colloidal systems and the potential impact of these on the thickness of the interfacial barriers that they can create, the soft matter nature of the biopolymer assemblies provides them with a unique interfacial advantage over harder particles. Microgel particles, for example, have been known to, amongst others, exhibit great deformability once positioned at liquid interfaces [48]. This can lead to the formation of highly dense barriers around emulsion droplets [48]. Although this has been principally studied in terms of emulsion stability provision [49], it should also impact on the rate of interfacial transportation and thus on release phenomena. It could be argued that if the biopolymer assemblies studied here possess some level of deformability, this would enable them to form dense interfaces that exhibit lower interfacial transport rates than those populated by inflexible particles such as colloidal silica.

## 4. Conclusions

The present work explores a range of food-relevant emulsifiers known to form colloidal particulates. The emulsifying performance of these species is firstly discussed, and it is highlighted that equilibrium interfacial tension is not necessarily the most appropriate predictor of final average droplet size obtained via high shear mixing. Instead, a measure of dynamic interfacial tension is recommended, in line with the timescales of droplet formation and coalescence phenomena experienced during processing. Further evidence for the propensity of protein/polysaccharide complexes to provide stable emulsions is also presented and the superiority of these structures over those formed via a layer-by-layer deposition approach is demonstrated. The same series of emulsifier species are also studied in terms of their capacity to modulate the release of a model hydrophobic active (DMP). The rate of DMP molecular release from the internal phase of an emulsion is shown to be controlled, to some extent, by the emulsifier chosen to stabilise the interface of the system. However, emulsions stabilised by hard inorganic particles do not always offer the slowest release. Depending on the protein component utilised, protein/polysaccharide complexes are shown to be more effective than hydrophilic silica nanoparticles. Even then, the lowest rate constant is provided by the SSL-stabilised emulsions; this is hypothesised to be a consequence of bi- or multilayer aggregate formation at the SSL interface.

Overall, the present study promotes current understanding onto how emulsion microstructure, and more specifically interfacial architecture, can be controlled to arrive at tailored molecular release capabilities. Although directly relevant to foods, the ability to enable controlled release functionality into emulsions using non-toxic, biodegradable structuring materials, such as those presented in this work, is becoming increasingly important in many other research settings. Previous work [11],[50] has shown that sintering and cross-linking of species at the interface can be employed to control the rate of active release from emulsions. Future research in this area would benefit from further development of quantitative relationships between interfacial material characteristics (e.g. interfacial rheology) and the corresponding release rate performance.

## Acknowledgements

The authors would also like to thank the Engineering and Physical Research Council (EPSRC, UK), Innovate UK (UK) and Syngenta for funding the work presented here. The authors would also like to thank Pat Mulqueen at Syngenta (Jealott's Hill International Research Centre) for useful discussions.

## References

[1] Madene A., Jacquot M., Scher J., Desobry S., 2006. Flavour Encapsulation and Controlled Release – A review. *International Journal of Food Science & Technology*, **41**: 1-21.

[2] Mohan A., Rajendran S.R.C.K., He Q.S., Bazinet L., Udenigwe C.C., 2015. Encapsulation of food protein hydrolysates and peptides: A review. *RSC Advances*, **5**(97): 79270-79278.

[3] Shchukin D.G., Grigoriev D.O., Möhwald H., 2010. Application of Smart Organic Nanocontainers in Feedback Active Coatings. *Soft Matter*, **6**: 720-725.

[4] Spyropoulos F., Kurukji D., Taylor P., Norton I.T., 2018. Fabrication and Utilization of Bifunctional Protein/Polysaccharide Coprecipitates for the Independent Codelivery of Two Model Actives from Simple Oil-in-Water Emulsions. Langmuir, **34**(13): 3934-3948.

[5] Dickinson E., 2010. Food Emulsions and Foams: Stabilization by Particles. *Current Opinion in Colloid & Interface Science*, **15**: 40-49.

[6] Dickinson E., 2009. Hydrocolloids as Emulsifiers and Emulsion Stabilizers. *Food Hydrocolloids*, **23**: 1473-1482.

[7] Quintero Quiroz J. Rojas J., Ciro G., 2018. Vegetable Proteins as Potential Encapsulation Agents: A review. *Food Research*, **2**: 208-220.

[8] Al-Omran M.F., Al-Suwayeh S.A., El-Helw A.M., Saleh S.I., 2002. Taste Masking of Diclofenac Sodium Using Microencapsulation. *Journal of Microencapsulation*, **19**: 45-52.

[9] Gibbs B.F., Kermasha S., Alli I., Mulligan C.N., 1999. Encapsulation in the food industry: A review. *International Journal of Food Sciences and Nutrition*, **50**(3): 213-224

[10] Simovic S., Prestidge C.A., 2007. Nanoparticle Layers Controlling Drug Release from Emulsions. *European Journal of Pharmaceutics and Biopharmaceutics*, **67**: 39-47.

[11] Frasch-Melnik S., Norton I.T., Spyropoulos F., 2010. Fat-Crystal Stabilised W/O Emulsions for Controlled Salt Release. *Journal of Food Engineering*, **98**: 437-442.

[12] Garrec D.A., Frasch-Melni, S., Henry J.V.L., Spyropoulos F., Norton I.T., 2012. Designing colloidal structures for micro and macro nutrient content and release in foods. *Faraday Discussions*, **158**: 37-49.

[13] Pawlik A., Kurukji D., Norton I.T., Spyropoulos F., 2016. Food-Grade Pickering Emulsions Stabilised with Solid Lipid Particles. *Food & Function*, **7**: 2712-2721.

[14] Ghosh S., Rousseau D., 2011. Fat Crystals and Water-in-Oil Emulsion Stability. *Current Opinion in Colloid & Interface Science*, **16**: 421-431.

[15] Wang L.-Y., Gu Y.-H., Zhou Q.-Z., Ma G.-H., Wan Y.-H., Su Z.-G., 2006. Preparation and Characterization of Uniform-Sized Chitosan Microspheres Containing Insulin by Membrane Emulsification and a Two-Step Solidification Process. *Colloids and Surfaces B: Biointerfaces*, **50**: 126-135.

[16] Sato A.C.K., Perrechil F.A., Costa A.A.S., Santana R.C., Cunha R.L., 2015. Cross-Linking Proteins by Laccase: Effects on the Droplet Size and Rheology of Emulsions Stabilized by Sodium Caseinate. *Food Research International*, **75**: 244-251.

[17] Aoki T., Decker E.A., McClements D.J., 2005. Influence of Environmental Stresses on Stability of O/W Emulsions Containing Droplets Stabilized by Multilayered Membranes Produced by a Layer-by-Layer Electrostatic Deposition Technique. *Food Hydrocolloids*, **19**: 209-220.

[18] Kokelaar J.J., Garritsen J.A., Prins A., 1995. Surface Rheological Properties of Sodium Stearoyl-2-Lactylate (SSL) and Diacetyl Tartaric Esters of Mono (and Di) Glyceride (Datem) Surfactants after a Mechanical Surface Treatment in Relation to Their Bread Improving Abilities. *Colloids and Surfaces A: Physicochemical and Engineering Aspects*, **95**: 69-77.

[19] Husband F.A., Ridout M.J., Clegg P.S., Hermes M., Forth J., Poon W.C.K., Wilde P.J., 2014. The Impact of the Interfacial Behaviour on Emulsion Rheology: A Potential Approach to Reducing Fat Content in Emulsified Foods. In: *Gums and Stabilisers for the Food Industry 17: The Changing Face of Food Manufacture: The Role of Hydrocolloids*, P.A. Williams, G.O. Phillips (Eds.), RSC: Cambridge, 230-237.

[20] Washington C., Evans K., 1995. Release rate measurements of model hydrophobic solutes from submicron triglyceride emulsions. *Journal of Controlled Release*, **33**(3): 383-390.

[21] Kurukji D., Pichot R., Spyropoulos F., Norton I.T., 2013. Interfacial Behaviour of Sodium Stearoyllactylate (SSL) as an Oil-in-Water Pickering Emulsion Stabiliser. *Journal of Colloid and Interface Science*, **409**: 88-97.

[22] Kurukji D., Norton I.T., Spyropoulos F., 2016. Fabrication of Sub-Micron Protein-Chitosan Electrostatic Complexes for Encapsulation and pH-Modulated Delivery of Model Hydrophilic Active Compounds. *Food Hydrocolloids*, **53**: 249-260.

[23] Borzova V.A., Markossian K.A., Chebotareva N.A., Kleymenov S.Y., Poliansky N.B., Muranov K.O., Stein-Margolina V.A., Shubin V.V., Markov D.I., Kurganov B.I., 2016. Kinetics of Thermal Denaturation and Aggregation of Bovine Serum Albumin. *PLoS One*, **11**: e0153495-e0153495.

[24] Pichot R., Spyropoulos F., Norton I.T., 2009. Mixed-Emulsifier Stabilised Emulsions: Investigation of the Effect of Monoolein and Hydrophilic Silica Particle Mixtures on the Stability against Coalescence. *Journal of Colloid and Interface Science*, **329**: 284-91.

[25] Pichot R., Spyropoulos F., Norton I.T., 2012. Competitive adsorption of surfactants and hydrophilic silica particles at the oil-water interface: Interfacial tension and contact angle studies. *Journal of Colloid and Interface Science*, **377**(1): 396-405.

[26] Washington C., 1989. Evaluation of Non-Sink Dialysis Methods for the Measurement of Drug Release from Colloids - Effects of Drug Partition. *International Journal of Pharmaceutics*, **56**: 71-74.

[27] Sasaki H., Takakura Y., Hashida M., Kimura T., Sezaki H., 1984. Antitumor Activity of Lipophilic Prodrugs of Mitomycin C Entrapped in Liposome or O/W Emulsion. *Journal of Pharmacobio-Dynamics*, **7**: 120-130.

[28] Dowding P.J., Atkin R., Vincent B., Bouillot P., 2005. Oil Core/Polymer Shell Microcapsules by Internal Phase Separation from Emulsion Droplets. II: Controlling the Release Profile of Active Molecules. *Langmuir*, **21**: 5278-5284.

[29] Zoldesi C.I., Imhof A., 2005. Synthesis of Monodisperse Colloidal Spheres, Capsules, and Microballoons by Emulsion Templating. *Advanced Materials*, **17**(7): 924-928.

[30] Guy R.H., Hadgraft J., Kellaway I.W., Taylor M.J., 1982. Calculations of drug release rates from particles. *International Journal of Pharmaceutics*, **11**(3): 199-207.

[31] Spyropoulos F., Duffus L.J., Smith P., Norton I.T., 2019. *Langmuir*, **35**(47): 15137-15150.

[32] Lloyd D., Norton I.T., Spyropoulos F., 2014. Processing Effects During Rotating Membrane Emulsification. *Journal of Membrane Science*, **466**: 8–17.

[33] Lloyd D., Norton I.T., Spyropoulos F., 2015. Process Optimisation of Rotating Membrane Emulsification through the Study of Surfactant Dispersions, *Journal of Food Engineering*, **166**: 316-324.

[34] Li G., Huang J., Chen T., Wang X., Zhang H., Chen Q., 2017. Insight into the interaction between chitosan and bovine serum albumin, *Carbohydrate Polymers*, **176**: 75-82.

[35] Ghosh S., Bull H.B., 1963. Adsorbed films of bovine serum albumin: Tensions at air-water surfaces and paraffin-water interfaces. *BBA - Biochimica et Biophysica Acta*, **66**(C): 150-157.

[36] Xi Y., Liu B., Jiang H., Yin S., Ngai T., Yang X., 2020. Sodium caseinate as a particulate emulsifier for making indefinitely recycled pH-responsive emulsions. *Chemical Science*, **11**(15): 3797-3803.

[37] Ma H., Forssell P., Partanen R., Seppänen R., Buchert J., Boer H., 2009. Sodium caseinates with an altered isoelectric point as emulsifiers in oil/water systems. *Journal of Agricultural and Food Chemistry*, **57**(9): 3800-3807.

[38] Zafeiri I., Norton J.E., Smith P., Norton I.T., Spyropoulos F., 2017. The role of surface active species in the fabrication and functionality of edible solid lipid particles. *Journal of Colloid and Interface Science*, **500**: 228-240.

[39] Payet L., Terentjev E.M., 2008. Emulsification and stabilization mechanisms of O/W emulsions in the presence of chitosan. *Langmuir*, **24**(21): 12247-12252.

[40] Nakauma M., Funami T., Noda S., Ishihara S., Al-Assaf S., Nishinari K., Phillips G.O., 2008. Comparison of Sugar Beet Pectin, Soybean Soluble Polysaccharide, and Gum Arabic as Food Emulsifiers. 1. Effect of Concentration, pH, and Salts on the Emulsifying Properties. *Food Hydrocolloids*, **22**: 1254-1267.

[41] Liu H., Wang C., Zou S., Wei Z., Tong Z., 2012. Simple, Reversible Emulsion System Switched by pH on the Basis of Chitosan without any Hydrophobic Modification. *Langmuir*, **28**: 11017-11024.

[42] Dickinson E., Pawlowsky K., 1997. Effect of ι-Carrageenan on Flocculation, Creaming, and Rheology of a Protein-Stabilized Emulsion. *Journal of Agricultural and Food Chemistry*, **45**: 3799-3806.

[43] Thanasukarn P., Pongsawatmanit R., McClements D.J., 2006. Utilization of Layer-by-Layer Interfacial Deposition Technique to Improve Freeze–Thaw Stability of Oil-in-Water Emulsions, *Food Research International*, **39**: 721-729.

[44] Barbosa L.R.S., Grazia Ortore M., Spinozzi F., Mariani P., Bernstorff S., Itri R., 2010. The Importance of Protein-Protein Interactions on the pH-Induced Conformational Changes of Bovine Serum Albumin: A Small-Angle X-Ray Scattering Study. Biophysical Journal, 98: 147-157.

[45] Murray B.S., Dickinson E., 1996. Interfacial Rheology and the Dynamic Properties of Adsorbed Films of Food Proteins and Surfactants. *Food Science and Technology International, Tokyo*, **2**(3): 131-145.

[46] Er Y., Barnes T.J., Fornasiero D., Prestidge, C.A., 2009. The encapsulation and release of guanosine from PEGylated liposomes. *Journal of Liposome Research*, **19**(1): 29-36.

[47] Shen J., Burgess D.J., 2012. Accelerated in Vitro Release Testing of Implantable PLGA Microsphere/PVA Hydrogel Composite Coatings. *International Journal of Pharmaceutics*, **422**: 341-348.

[48] Deshmukh O.S., Van Den Ende D., Stuart M.C., Mugele F., Duits M.H.G., 2015. Hard and soft colloids at fluid interfaces: Adsorption, interactions, assembly & rheology. *Advances in Colloid and Interface Science*, **222**: 215-227.

[49] Schmidt S., Liu T., Rütten S., Phan K.-H., Möller M., Richtering W., 2011. Influence of microgel architecture and oil polarity on stabilization of emulsions by stimuli-sensitive core-shell poly(N-isopropylacrylamide-co-methacrylic acid) microgels: Mickering versus Pickering behavior? *Langmuir*, **27**(16): 9801-9806.

[50] Yow H.N., Routh A.F., 2009. Release Profiles of Encapsulated Actives from Colloidosomes Sintered for Various Durations. *Langmuir*, **25**, 159-166.